Publication VII

Xiaomeng Liu, Arja-Helena Vesterinen, Jan Genzer, Jukka V. Seppälä, and Orlando J. Rojas. 2011. Adsorption of PEO–PPO–PEO triblock copolymers with end-capped cationic chains of poly(2-dimethylaminoethyl methacrylate). Langmuir, volume 27, number 16, pages 9769-9780.

Langmuir

ARTICLE

pubs.acs.org/Langmuir

Adsorption of PEO−PPO−PEO Triblock Copolymers with End-Capped Cationic Chains of Poly(2-dimethylaminoethyl methacrylate)

Xiaomeng Liu,[†] Arja-Helena Vesterinen,[§] Jan Genzer,[‡] Jukka V. Seppälä,[§] and Orlando J. Rojas*[,†,∥]

[†]Department of Forest Biomaterials and [‡]Department of Chemical & Bimolecular Engineering, North Carolina State University, Raleigh, North Carolina 27695, United States

[§]Faculty of Chemistry and Materials Sciences, Department of Biotechnology and Chemical Technology, Aalto University, P.O. Box 16100, FI-00076 Aalto, Finland

[∥]Faculty of Chemistry and Materials Sciences, Department of Forest Products Technology, Aalto University, P.O. Box 16300, FI-00076, Aalto, Finland

Supporting Information

ABSTRACT: We study the adsorption of a symmetric triblock copolymer of ethylene oxide, EO, and propylene oxide, PO, end-capped with quarternized poly(2-dimethylaminoethyl methacrylate), DMAEMA ($DMAEMA_{24}$−$EO_{132}PO_{50}EO_{132}$−$DMAEMA_{24}$). Light scattering and tensiometry are used to measure the relative size of the associated structures and surface excess at the air−liquid interface. The adsorbed amount, the amount of coupled water, and the viscoelasticity of the adsorbed polymer layer are measured on hydrophobic and hydrophilic surfaces (polypropylene, cellulose, and silica) by using quartz crystal microgravimetry (QCM) and surface plasmon resonance (SPR) at different ionic strengths and temperatures. The results of the experiments are compared with those obtained after adsorption of the uncharged precursor copolymer, without the cationic end-caps ($EO_{132}PO_{50}EO_{132}$). $DMAEMA_{24}$−$EO_{132}PO_{50}EO_{132}$−$DMAEMA_{24}$ possesses higher affinity with the negatively charged silica and cellulose surfaces while the uncharged copolymer adsorbs to a larger extent on polypropylene surfaces. In this latter case, adsorption increases with increasing solution ionic strength and temperature. Adsorption of $EO_{132}PO_{50}EO_{132}$ on silica surfaces has little effect on the water contact angle (WCA), while adsorption of $DMAEMA_{24}$−$EO_{132}PO_{50}EO_{132}$−$DMAEMA_{24}$ increases the WCA of silica to 32°, indicating a large density of exposed PPO blocks upon adsorption. After adsorption of $EO_{132}PO_{50}EO_{132}$ and $DMAEMA_{24}$−$EO_{132}PO_{50}EO_{132}$−$DMAEMA_{24}$ on PP, the WCA is reduced by ≈14° and ≈28°, respectively, due to the exposed hydrophilic EO and highly water-soluble DMAEMA segments on the surfaces. The extent of surface coverage at saturation at the polypropylene/liquid interfaces (≈31 and 40 nm^2/molecule obtained by QCM and SPR, respectively) is much lower, as expected, when compared with results obtained at the air/liquid interface, where a tighter packing is observed. The percentage of water coupled to the adsorbed cationic polymer decreases with solution ionic strength. Overall, these observations are ascribed to the effects of electrostatic screening, polymer hydrodynamic size, and solvency.

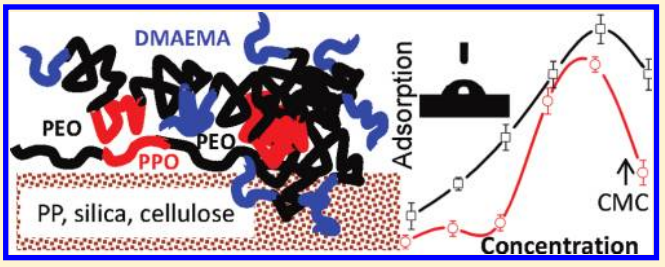

INTRODUCTION

Adsorption of polymers at solid−liquid interfaces is critical in modifying the interfacial properties of a variety of industrial products, including detergents,[1] colloidal dispersants and stabilizers,[2] lubricants, and hydrophilizing/hydrophobizing agents. Pluronics are commercially available water-soluble nonionic triblock copolymers made of poly(propylene oxide) (PO) and poly(ethylene oxide) (EO) blocks with varying block sizes, i.e., $(\text{ethylene oxide})_n$−$(\text{propylene oxide})_m$−$(\text{ethylene oxide})_n$ $[(EO)_n(PO)_m(EO)_n]$. These systems have been the subject of many studies dealing with fundamental aspects of adsorption on solid surfaces.[3−8] Charged and thermoresponsive polymers, such as poly(2-dimethylaminoethyl methacrylate) (PDMAEMA), have attracted interest due to their responsiveness to variations in pH and temperature. These characteristics make PDMAEMA (and other macromolecules with similar properties) useful in drug delivery, bioseparation, and microfluidic applications.[9−11] Quarternized PDMAEMA has been considered to be a suitable candidate for the development of cationic antimicrobial surfaces, among others.[12−14] In addition, it has been reported that water-soluble amphiphilic block polyelectrolytes carrying PDMAEMA chains can potentially be utilized to modify the wetting properties of charged surfaces.[15]

Block copolymers of $(EO)_n(PO)_m(EO)_n$ end-capped with quaternized PDMAEMA groups, as reported recently,[16] are expected to exhibit several of the main features of the precursor Pluronic-type macromolecules. These macromolecules also exhibit better solubility, higher affinity with oppositely charged

Received: April 29, 2011
Revised: June 29, 2011
Published: July 02, 2011

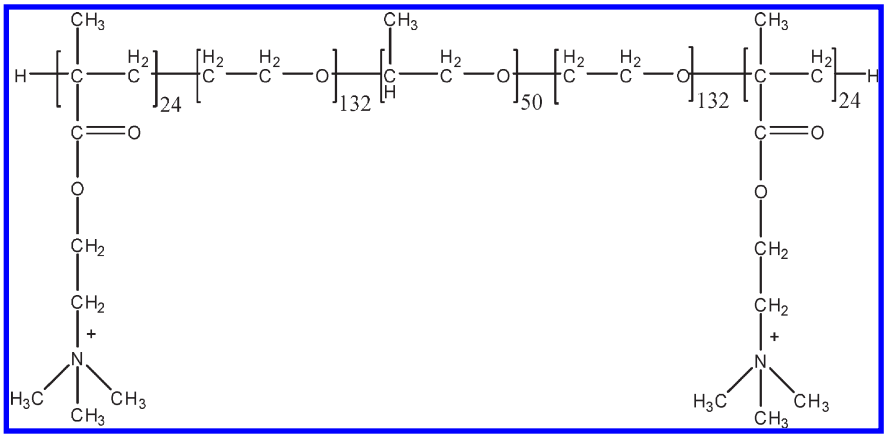

Figure 1. Chemical formula of EO−PO−EO triblock copolymers with end-capped cationic chains of poly[2-dimethylamino]ethyl methacrylate] ($DMAEMA_{24}$−$EO_{132}PO_{50}EO_{132}$−$DMAEMA_{24}$).

surfaces, antimicrobial activity, and can be suitably modified to tune the wetting properties of hydrophobic and charged surfaces. While the physical properties of $(EO)_n(PO)_m(EO)_n$ end-capped with PDMAEMA have been reported,[16] their solution and adsorption behaviors are yet to be elucidated.

The aim of this study are (1) to investigate the interactions, degree of hydration, adsorbed mass, and viscoelasticity of a copolymer of PEO−PPO−PEO end-capped with PDMAEMA upon adsorption onto various solid surfaces and (2) to compare the results with those after adsorption of the same copolymer but without the end-caps. Surface tension isotherms and light scattering for the two block copolymers are presented followed by discussion pertaining to polymer adsorption on substrates of different hydrophilicity and charge. Quartz crystal microbalance (QCM) and surface plasmon resonance (SPR) techniques are employed in tandem to study the effects on adsorption of aqueous solution ionic strength and temperature. Finally, the changes in surface wetting upon polymer adsorption are also presented.

MATERIALS AND METHODS

Deionized (DI) water from an ion-exchange system (Pureflow, Inc.) followed by filtration in a Milli-Q Gradient unit with a resultant resistivity of >18 MΩ cm was used to prepare the polymer solutions and was also employed in QCM and SPR experiments (background fluid, rinsing solution, etc.). A symmetrical triblock nonionic copolymer consisting of polyethylene oxide and polypropylene oxide blocks with a theoretical weight-average molecular weight of 14.6 kDa was donated by BASF Corp. under the trade name of Pluronic F108 ($EO_{132}PO_{50}EO_{132}$) and was used without further purification. The cloud point and solubility in aqueous solution of $EO_{132}PO_{50}EO_{132}$ were determined to be >100 °C and >10%, respectively. The same polymer with quaternized PDMAEMA end chains was synthesized; details about its bulk and solution properties can be found in ref 16. The molecular weight of PDMAEMA blocks was ≈7.4 kDa (equivalent to 24 DMAEMA units). The number-average molecular weight and polydispersity index of $DMAEMA_{24}$−$EO_{132}PO_{50}EO_{132}$−$DMAEMA_{24}$ were determined by size-exclusion chromatography to be 32.3 kDa and 1.5, respectively.[16] Amino groups in these polymers were further modified into ammonium according to the procedure described earlier.[17] The structure of the end-capped copolymer is shown in Figure 1. Aqueous solutions of $EO_{132}PO_{50}EO_{132}$ and $DMAEMA_{24}$−$EO_{132}PO_{50}EO_{132}$−$DMAEMA_{24}$ were freshly prepared at concentrations ranging from 1×10^{-3} to 10 w/v % before each experiment.

Quartz sensors coated with gold as well as silica (Biolin Scientific AB, Sweden) were used in QCM experiments. Gold-coated slides (Oy BioNavis Ltd., Tampere, Finland) were also used in experiments with surface plasmon resonance (SPR). These sensors were treated first with piranha solution [70% H_2SO_4 + 30% H_2O_2 (30%)] for 20 min followed by UV/ozone treatment (28 mW/cm^2) for 10 min to remove any organic contaminants. Thin films of PP and cellulose were deposited on the cleaned QCM and SPR gold sensors by spin-coating; details about their manufacture can be found in ref 18.

Surface Tension. The surface tension of aqueous solutions of $EO_{132}PO_{50}EO_{132}$ and $DMAEMA_{24}$−$EO_{132}PO_{50}EO_{132}$−$DMAEMA_{24}$ was measured at 25 °C by using a Cahn balance (Thermo Material Characterization, Madison, WI) equipped with a Pt−Ir Willhelmy plate. The minimum surface tension and the critical micelle concentration (cmc) were determined.

Dynamic Light Scattering. The hydrodynamic radii of the polymers in aqueous solution (0.0001, 0.001, 0.01, 0.1, 1, and 10 w/v % concentration) were measured with Zetasizer Nano ZS dynamic light scattering (DLS) equipment at a 173° scattering angle. In addition, NaCl concentrations of 100 and 1000 mM NaCl were used in the case of 0.1 w/v % polymer aqueous solutions. Prior to the respective measurement, the samples were filtered with 0.45 μm syringe filters. Each measurement consisted of 33 scans during 10 s; three repetitions were performed for each sample. Attenuator 10 was used in all measurements. The experiments were conducted at 25 and 40 °C, and the stabilization time before measurement was 5 (25 °C) or 60 min (40 °C).

Quartz Crystal Microbalance. A quartz crystal microbalance (Q-Sense model E4, Biolin Scientific AB, Sweden) was used to measure the rate of adsorption, the adsorbed mass, and viscoelasticity of the adsorbed layers. The principle of QCM has been described in detail elsewhere.[19] In short, changes in the resonant frequency Δf and energy dissipation ΔD of the coated QCM sensors were measured simultaneously by switching on and off the applied voltage. The shift in the resonant frequency due to polymer adsorption was employed to calculate the areal adsorption (Δm) by means of the Sauerbrey equation (eq 1),[20] which is generally applicable if (1) the adsorbed macromolecules form a thin, rigid, and homogeneous layer and (2) the adsorbed mass is small compared to that of the QCM sensor or resonator

$$\Delta m = -c\frac{\Delta f}{n} \quad (1)$$

where n is the overtone number (n = 1, 3, 5, 7, etc.) and c is a characteristic constant related to the sensitivity of the resonator to changes in mass [c = 17.7 ng Hz^{-1} cm^{-2} for the quartz crystals at the fundamental (n = 1) frequency of 5 MHz].

dx.doi.org/10.1021/la201596x |*Langmuir* 2011, 27, 9769–9780

The shift in the QCM energy dissipation, ΔD, was used to determine changes in the viscoelastic properties of the adsorbed layer. ΔD was measured after switching off the resonator and by recording the exponential decay in oscillation (frequency and amplitude dampening), which were then used to obtain the energy dissipated and stored during one period of oscillation, $E_{\text{dissipated}}$ and E_{stored}, respectively, according to eq 2:

$$D = \frac{E_{\text{dissipated}}}{2\pi E_{\text{stored}}} \tag{2}$$

The energy dissipation is attributed to changes in viscoelastic properties of the crystal and adsorbed layer and to variations in the density and viscosity of the surrounding solution.[21] Therefore, changes in f and D were recorded after a rinsing step to replace the adsorbing polymer solution with polymer-free solution, thereby allowing the determination of effective changes.

The QCM modules and tubing were cleaned for 1 h before each run by using a 2% (v/v) Hellmanex solution (Hellma GMBH, Müllheim, Germany). They were then rinsed with ethanol and water. After mounting the respective coated sensor in the QCM module, water was injected continuously with the system adjusted to a temperature of 25 ± 0.02 °C. In a typical experiment, uniform ultrathin films of polypropylene (PP) and cellulose were first deposited on the QCM gold sensors by spin-coating. The thicknesses and roughness of the respective thin films, under the same operating conditions, were reported in our previous publication.[18] The shifts in the QCM frequency both in air and in water media were used to test the quality of the coating before each experiment.

Prior to any measurement, the coated sensors were allowed to equilibrate in water for half a day in order to establish the base f and D signals, which were then zeroed. In order to study the adsorption of $EO_{132}PO_{50}EO_{132}$ and $DMAEMA_{24}-EO_{132}PO_{50}EO_{132}-DMAEMA_{24}$, aqueous solutions of these polymers, with concentration in the range from 1×10^{-3} to 10 w/v %, were injected into the QCM module using a constant flow rate of 0.1 mL/min. The shifts in f and D were monitored as a function of time up to ≈15 min, followed by rinsing with background solution (either water or NaCl aqueous solution). Continuous injection of polymer at increased concentrations was found to produce similar adsorption results compared to those after single injections. In this work, we report only adsorption data obtained by running single experiments, at the given polymer concentration. All adsorption experiments were conducted in triplicate and average values reported.

Surface Plasmon Resonance. Polymer adsorption was also investigated by surface plasmon resonance (SPR) (SPR Navi 200, Oy BioNavis Ltd., Tampere, Finland). The superb sensitivity of electromagnetic plasmon waves, which propagate along the interface between a metallic (Au) substrate and the surrounding medium, to any variation at the interface is ideally suited for detecting molecular adsorption.[22] The changes in optical resonance at the interface can be determined by the specific angle shift at which the reflected light intensity was minimum. Therefore, the SPR signal, expressed in resonance units or in angle shift ($\Delta\theta$) can be used to determine the mass adsorbed on the sensor surface.[20] When the thickness of the adsorbed layer is much less than the wavelength of the probing laser, the shift in the adsorbed mass (Δm_{SPR}) can be calculated by using eq 3[23]

$$\Delta m_{\text{SPR}} = \frac{l_{\text{decay}}}{2}\frac{dc}{dn}\kappa\Delta\theta \tag{3}$$

where κ is the sensitivity factor of the system which relates the change in $\Delta\theta$ to the variation of the refractive index n within the evanescent field; dc/dn is the reverse of the refractive index increment with concentration c, l_{decay} is the decay length of the evanescent field (instrument-dependent), and c is the solution concentration. In the present case, the adsorption was measured in SPR as the variation of intensity of surface plasmons excited by the external light source.

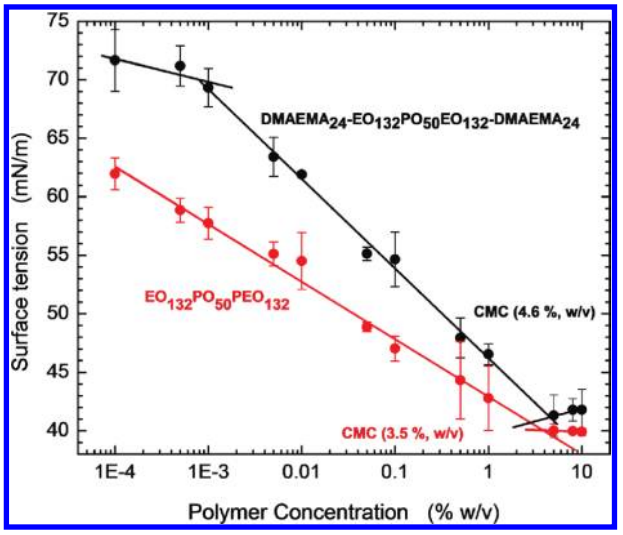

Figure 2. Surface tension isotherm in salt-free aqueous solutions of $EO_{132}PO_{50}EO_{132}$ and $DMAEMA_{24}-EO_{132}PO_{50}EO_{132}-DMAEMA_{24}$ measured at 25 °C. The solid lines are added as a guide to the eye.

The sensitivity factor of the SPR instrument used in this work was obtained by calculating the slope of a $\Delta\theta$ calibration curve for a series of glycerin aqueous solutions in the range of concentrations between 0.1 and 10% (v/v) and known refractive indices.[24] The SPR experiments were performed under the same set of conditions (polymer solution concentration, temperature, flow rate, rinsing protocol, etc.) as those used in the QCM experiments so that information on adsorption and desorption behaviors could be compared. The main difference between QCM and SPR is that the QCM frequency shifts depends on the total oscillating mass, including water coupled to the adsorbed molecules, while for SPR the refractivity is not affected by bound water molecules.[25] Hence, by calculating the adsorbed mass from QCM (Δm_{QCM}) and SPR (Δm_{SPR}) the contribution of water coupled or solvating the adsorbed layer could be evaluated, as shown in eq 4:

$$\%\text{coupled water} = \left(\frac{\Delta m_{\text{QCM}} - \Delta m_{\text{SPR}}}{\Delta m_{\text{QCM}}}\right) \times 100 \tag{4}$$

Water Contact Angle. Advancing water contact angles on the different surfaces were measured using a model 200 Ramé-Hart contact angle goniometer (Ramé-Hart Instrument Co., Netcong, NJ). The contact angles of the polymer substrates were assessed both before and after adsorption of $EO_{132}PO_{50}EO_{132}$ and $DMAEMA_{24}-EO_{132}PO_{50}EO_{132}-DMAEMA_{24}$ from aqueous solutions of 0.1% w/v concentration. All samples were dried by blowing air for 1 min right before contact angle measurements. The advancing contact angles were obtained after numerical solution of the full Young−Laplace equation of the shape of a sessile drop (5 μL) by slowly increasing (0.02 μL/s) its volume with a thin needle. The contact angles were measured within 1 h after the sample was prepared on at least four different locations on the surface.

RESULTS AND DISCUSSION

Surface Tension and Critical Micelle Concentration (cmc). Figure 2 shows the surface tension isotherm of aqueous solutions of $EO_{132}PO_{50}EO_{132}$. The change in the surface tension slope indicated a critical micelle concentration (cmc) of 3.5% w/v,

dx.doi.org/10.1021/la201596x |Langmuir 2011, 27, 9769–9780

Table 1. Light Scattering Intensity and Macromolecule Size of Aqueous Solutions in the Range of Concentrations between 0.0001 and 10% w/v of $EO_{132}PO_{50}EO_{132}$ (P) and $DMAEMA_{24}$−$EO_{132}PO_{50}EO_{132}$−$DMAEMA_{24}$ (C−P) Measured at 25 and 40 °C

	T = 25 °C				T = 40 °C			
	LS intensity (au)		size (nm)		LS intensity (au)		size (nm)	
%	P	C−P	P	C−P	P	C−P	P	C−P
10	234	221	15	50	878	475	14	18
1	82	15	7	3	977	28	9	11
0.1	31	33	4	4	121	16	7	3
0.01	42	9	u[a]	u	16	17	u	u
0.001	8	21	u	u	11	15	u	u
0.0001	14	9	u	u	10	7	u	u

[a] "u" indicates unimer.

in close agreement with values from light scattering measurements and reports by other authors.[26] It has been proposed that at this concentration $EO_{132}PO_{50}EO_{132}$ macromolecules associate to form micelles.[27] The slight reduction in surface tension after the cmc was indicative of the anticipated mass or size dispersity of the molecule. Figure 2 also shows the surface tension isotherm of aqueous solutions of $DMAEMA_{24}$−$EO_{132}PO_{50}EO_{132}$−$DMAEMA_{24}$. A cmc value of 4.6% w/v was determined which appears to be close to that for the uncharged $EO_{132}PO_{50}EO_{132}$ polymer. The slightly higher value of cmc for the charged polymer can be explained by the reduced hydrophobic effect (and better solvency) and by the fact that polymer association was limited due to electrostatic repulsion.

The surface excess Γ at the air/liquid interface was obtained by the Gibbs adsorption equation for nonionic surfactants (eq 5)

$$\Gamma = -\frac{1}{RT}\left(\frac{\partial\gamma}{\partial \ln c}\right)_T \quad (5)$$

where γ is the surface tension, in the present case measured at 298.2 K; R is the universal gas constant, and c is the polymer molar concentration. At maximum $EO_{132}PO_{50}EO_{132}$ and $DMAEMA_{24}$−$EO_{132}PO_{50}EO_{132}$−$DMAEMA_{24}$ packing the calculated surface excess was 0.51 and 0.625 molecules/nm^2, respectively (1240 and 8560 ng/cm^2). These values are noted here as a reference for further discussions in the context of the areal adsorption determined at solid−liquid interfaces.

Light Scattering (LS). Scattering intensity depends both on the aggregate size and polymer concentration (number of scatters). Scattering intensity should increase linearly with increasing concentration as long as no aggregation occurs. Therefore, aggregation can be observed as a sharp increase in scattering intensity. Table 1 shows the LS intensity and macromolecule size in aqueous solutions of $DMAEMA_{24}$−$EO_{132}PO_{50}EO_{132}$−$DMAEMA_{24}$ measured at 25 and 40 °C. The LS intensity values were found to be reproducible in repeated runs for $DMAEMA_{24}$−$EO_{132}PO_{50}EO_{132}$−$DMAEMA_{24}$. At submicellar concentrations, bimodality was observed, which indicated that both unimers and micelles were present in solution. This is reasonable since in dynamic polymer systems aggregation occurs at submicellar concentrations. We note that the polymer sizes could be reported most reliably at concentration above the cmc.

Table 2. Light Scattering Intensity of Aqueous Solutions (0.1% w/v) of $EO_{132}PO_{50}EO_{132}$ (P) and $DMAEMA_{24}$−$EO_{132}PO_{50}EO_{132}$−$PDMAEMA_{24}$ (C−P) at Various NaCl Concentrations (0, 100, 1000 mM) Measured at 25 and 40 °C

	LS intensity (au)			
	25 °C		40 °C	
NaCl (mM)	P	C−P	P	C−P
0	31	33	12	16
100	17	32	119	12
1000	35	15	284	7

No differences in the cmc values at the two temperatures tested were observed for the cationic block copolymer. However, at 40 °C, micellization of $EO_{132}PO_{50}EO_{132}$ started at lower concentration and the scattered light intensity increased more sharply when the cmc was reached. These effects are likely due to the limited solubility at high temperature of the PPO blocks of the nonionic polymer.[26]

For both $EO_{132}PO_{50}EO_{132}$ and $DMAEMA_{24}$−$EO_{132}PO_{50}EO_{132}$−$DMAEMA_{24}$ at submicellar concentrations, the LS intensity of the polymer solution was lower at 40 °C compared to that at 25 °C. This is indicative of the self-association and aggregation of the PPO blocks, which are more sensitive to temperature. In addition, at concentrations above the cmc, the macromolecular size was smaller at 40 °C compared to that at 25 °C, which was also most likely caused by the poorer solubility and the smaller hydrodynamic size of the PPO blocks.

Table 2 includes the light scattering intensity of submicellar (0.1% w/v) polymer solutions of different background NaCl concentrations (0, 100, and 1000 mMNaCl) at 25 and 40 °C. The light scattering intensity corresponds to the polymer coil size or the size of associated structures of $DMAEMA_{24}$−$EO_{132}PO_{50}EO_{132}$−$DMAEMA_{24}$. Scattering intensity of $DMAEMA_{24}$−$EO_{132}PO_{50}EO_{132}$−$DMAEMA_{24}$ decreased with increasing NaCl concentration at both temperatures. With addition of salt the electrostatic repulsion between cationic PDMAEMA groups decreased and the cationic PDMAEMA groups adopted a more coiled conformation. The same phenomenon was not seen with nonionic $EO_{132}PO_{50}EO_{132}$, in which case a sharp increase in intensity was observed at 40 °C. This is explained by a salt-induced micellization,[28] where the solubility of the polymer is reduced with increasing salt concentration. Thus, aggregation of $EO_{132}PO_{50}EO_{132}$ was driven by both temperature and ionic strength.

In the absence of salt, the intensity for both $EO_{132}PO_{50}EO_{132}$ and $DMAEMA_{24}$−$EO_{132}PO_{50}EO_{132}$−$DMAEMA_{24}$ decreased, which can possibly be due to the aggregation of the PPO segments.[26] With the addition of salt, the electrostatic intrachain repulsion decreased and there were higher probabilities for the cationic PDMAEMA block to ball up, forming a more compact, Gaussian-like chain. The repulsion among the cationic PDMAEMA groups and screening of electrostatic forces at increased ionic strengths explain the observed aggregation of the cationic molecules.

Adsorption of $EO_{132}PO_{50}EO_{132}$ and $DMAEMA_{24}$−$EO_{132}PO_{50}EO_{132}$−$DMAEMA_{24}$. Figure 3 shows QCM frequency shift vs time data illustrating the dynamics of the process of adsorption from aqueous solutions of $EO_{132}PO_{50}EO_{132}$ and

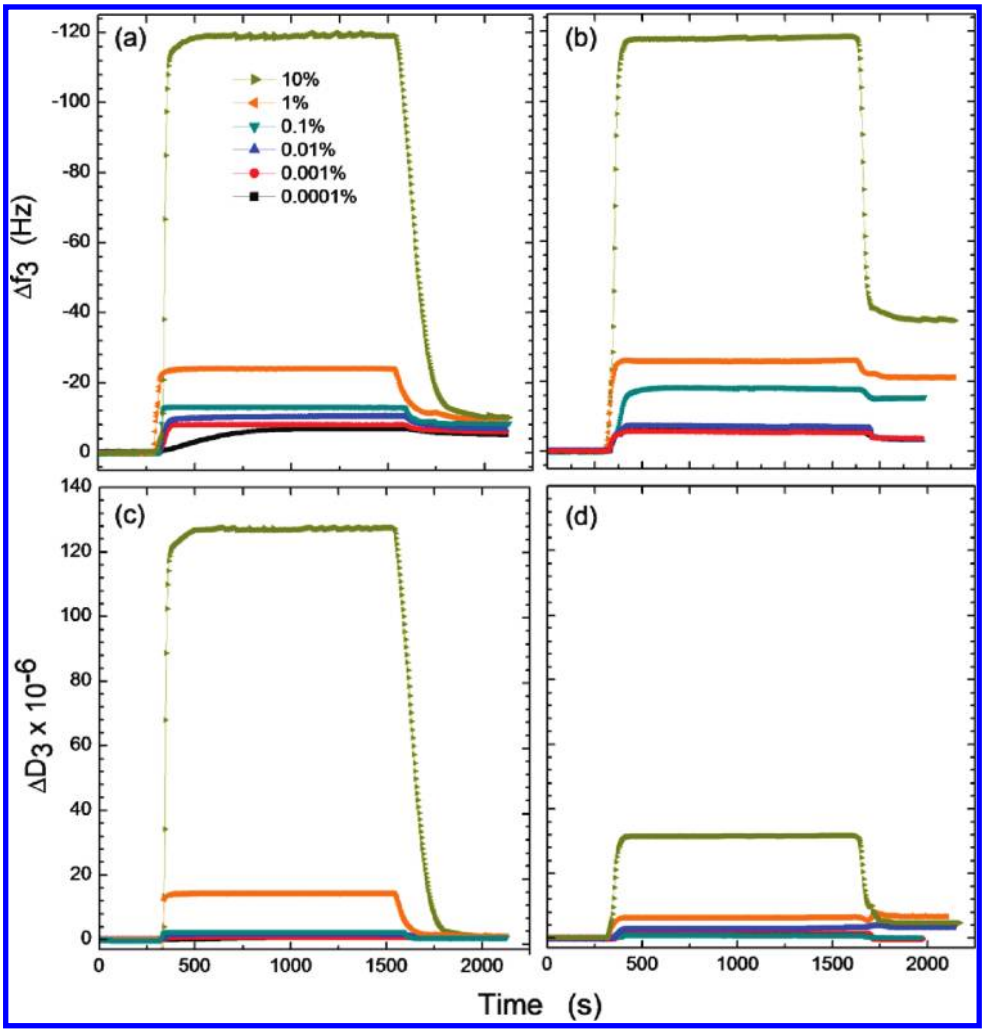

Figure 3. Mean values of third overtone QCM shifts in frequency (upper figures) and dissipation (bottom figures) as a function of time for $EO_{132}PO_{50}EO_{132}$ (a and c) and $DMAEMA_{24}-EO_{132}PO_{50}EO_{132}-DMAEMA_{24}$ (b and d) upon adsorption from aqueous solutions on silica surfaces at various aqueous solution concentrations (0.0001−10%, w/v). The experiments were conducted in an open (continuous) flow configuration with polymer solution injection rate of 0.1 mL/min (starting at about 300 s). The dip observed in all profiles soon after the adsorption plateau (at ≈1500−1750 s) was produced after rinsing the system with water. Upon rinsing, abrupt changes in frequency were observed until *f* and *D* reached constant values. The experiments were conducted at 25 ± 0.02 °C. Each curve represents the average of three independent measurements each performed with a different surface.

$DMAEMA_{24}-EO_{132}PO_{50}EO_{132}-DMAEMA_{24}$ on silica surfaces; isotherms showing similar trends were obtained when using PP and cellulose substrates (data not shown). In a typical adsorption experiment water was first injected continuously in the QCM sample loop until a stable *f* baseline was achieved. Thereafter, aqueous solutions of the respective polymer were introduced and sharp shifts in frequency and dissipation were observed (see Figure 3). These changes were indicative of fast mass uptake by the resonator due to the adsorption of the macromolecules. After the frequency and dissipation signals reached plateau values (typically in less than ≈10 min), water was introduced to remove any excess of loosely bound polymer. The recorded signals were used to measure the effective adsorption by comparing them with the baseline frequency and dissipation, in the absence of adsorbing polymer and under same bulk solution density and viscosity.

The frequency shifts in QCM, which can be converted to adsorbed mass, increased with increasing $EO_{132}PO_{50}EO_{132}$ and $DMAEMA_{24}-EO_{132}PO_{50}EO_{132}-DMAEMA_{24}$ solution concentration (Figures 3a,b). On the basis of these results and also from the solvency of the different polymer blocks (for example, as described by the Flory parameters[29]), the adsorption of $EO_{132}PO_{50}EO_{132}$ on silica surfaces likely occurred with the PEO segments anchoring to the surface while the PPO groups were solvated in the aqueous medium. It has been reported that silanol groups on the surface of silica facilitate the adsorption of PEO[30,31] as well as surfactants and block copolymers containing EO groups.[32] Furthermore, electrostatic interactions are likely to be a major driving mechanism for the adsorption of $DMAEMA_{24}-EO_{132}PO_{50}EO_{32}-DMAEMA_{24}$ on the negatively charged silica surfaces.[15] However, nonspecific adsorption of PEO groups on silica cannot be ruled out.

A modified Langmuir kinetic model as reported in ref 8 was found suitable to describe the dynamics of the adsorption of $EO_{132}PO_{50}EO_{132}$ and $DMAEMA_{24}-EO_{132}PO_{50}EO_{132}-DMAEMA_{24}$. The adsorption rate was found to depend on the

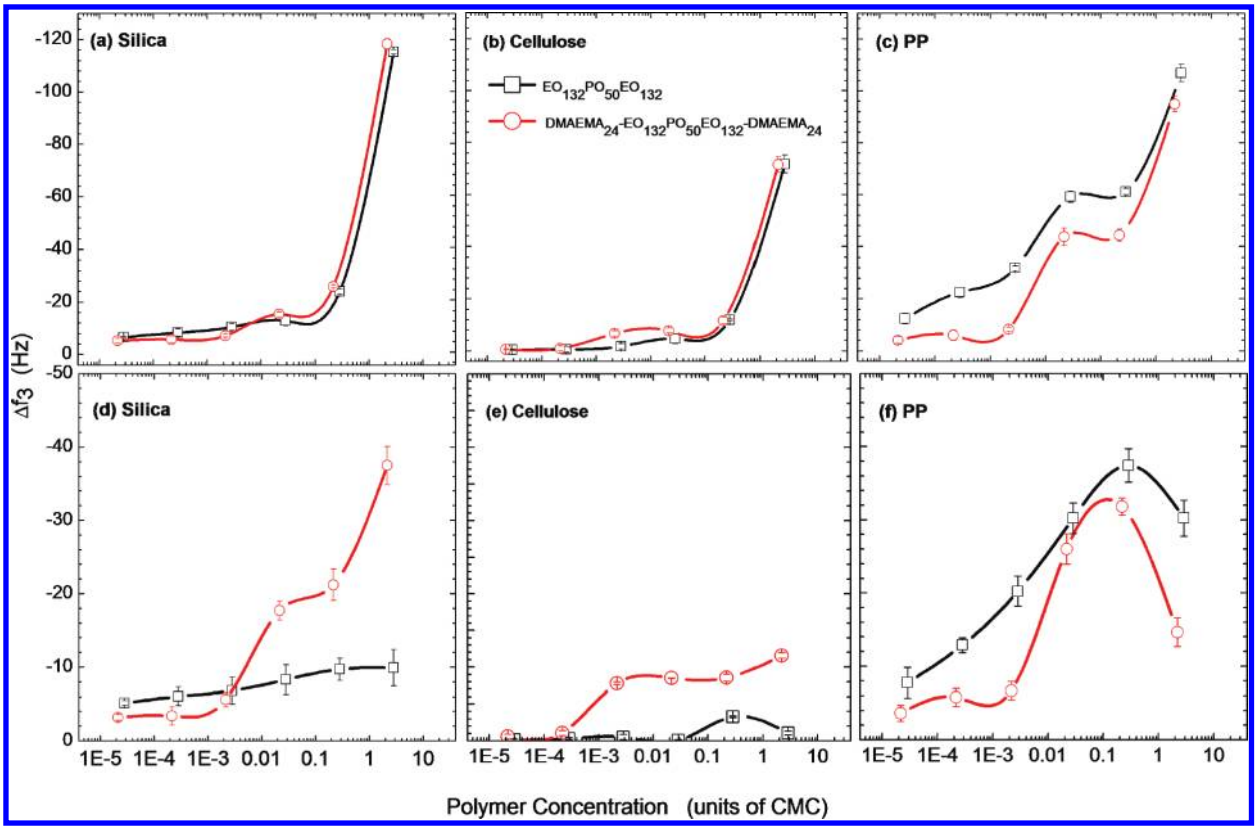

Figure 4. QCM frequency shift isotherms (25 ± 0.02 °C) as a function of polymer solution concentration upon adsorption of $EO_{132}PO_{50}EO_{132}$ (squares) and $DMAEMA_{24}-EO_{132}PO_{50}EO_{132}-DMAEMA_{24}$ (circles) onto silica, cellulose, and PP. Two sets of isotherms are included: before rinsing with water (reversible adsorption, upper panel) and after rinsing with water (irreversible adsorption, bottom panel). Each data point represents the average of three independent measurements each performed with a different surface. The error bars represent experimental standard deviations. The solid lines are added as a guide to the eye.

polymer concentration as was illustrated for the adsorption of $EO_{37}PO_{56}EO_{37}$.[8]

By comparing the results of adsorbed $EO_{132}PO_{50}EO_{132}$ and $DMAEMA_{24}-EO_{132}PO_{50}EO_{132}-DMAEMA_{24}$ after rinsing (irreversible adsorption), it is obvious that the adsorbed amount on silica was higher for cationic, PDMAEMA-capped polymer, especially at high polymer concentrations. This can be explained by the presence of the quaternary cationic groups (PDMAEMA) that adsorbed on the oppositely charged silica surface due to electrostatic interactions between the silanol groups on silica surfaces and the quarternized PDMAEMA blocks. However, it can be conjectured that having the adsorption blocks at the ends of the copolymer does not necessarily lead to increases in adsorption because of steric hindrance effects; the block copolymer may not utilize all space on the surface effectively and, as a result, a large density of loops and small density of trains may be expected.

The most striking difference between the adsorption of the two polymers is revealed by the changes that occurred in energy dissipation (D), as depicted in Figure 3c,d. Figure 3c suggests that $EO_{132}PO_{50}EO_{132}$ adsorbed as a loose, highly hydrated structure that was removed extensively upon rinsing with water. In contrast, the cationic polymer $DMAEMA_{24}-EO_{132}PO_{50}-EO_{132}-DMAEMA_{24}$ adsorbed more tightly to the surface. After rinsing with water both polymers exhibited the characteristics of relatively thin and rigid structures (the net dissipation shift was lower than 1×10^{-6} units). Furthermore, when the polymer concentration was close to or above the cmc, D was larger for $DMAEMA_{24}-EO_{132}PO_{50}EO_{132}-DMAEMA_{24}$ compared to that of $EO_{132}PO_{50}EO_{132}$, even after the adsorbed layer was rinsed with water. This behavior can be explained by the large amount of polymer adsorbed onto silica surfaces via electrostatic forces and hydrogen bonding. In addition, it is also possible that a large amount of water was coupled to the adsorbed $DMAEMA_{24}-EO_{132}PO_{50}EO_{132}-DMAEMA_{24}$ layer.

Figure 4 includes the QCM frequency isotherms of $EO_{132}PO_{50}EO_{132}$ and $DMAEMA_{24}-EO_{132}PO_{50}EO_{132}-DMAEMA_{24}$ adsorbed on silica, cellulose, and PP surfaces before and after rinsing with water. Rinsing did not lead to complete desorption of $EO_{132}PO_{50}EO_{132}$ and $DMAEMA_{24}-EO_{132}PO_{50}EO_{132}-DMAEMA_{24}$. In fact, while frequency shifts after rinsing indicated the removal of loosely bound molecules, a large number of segments remained adsorbed on the surface, likely due to an energy barrier that prevented their desorption. It has been reported that hydrophilic PEO blocks are most likely adsorbed from aqueous solution onto hydrophilic surfaces,[27] while on hydrophobic surfaces the adsorption is predominantly governed by the PPO blocks.[3] The cationic PDMAEMA groups are expected to adsorb on the negatively charged silica and cellulose surfaces.

The data in Figure 4 show that the adsorption of $EO_{132}PO_{50}EO_{132}$ and $DMAEMA_{24}-EO_{132}PO_{50}EO_{132}-DMAEMA_{24}$ onto the relatively hydrophobic (PP) surfaces resulted in large frequency shifts as a function of the solution polymer concentration (however, a maximum in adsorption around the cmc was

dx.doi.org/10.1021/la201596x |*Langmuir* 2011, 27, 9769–9780

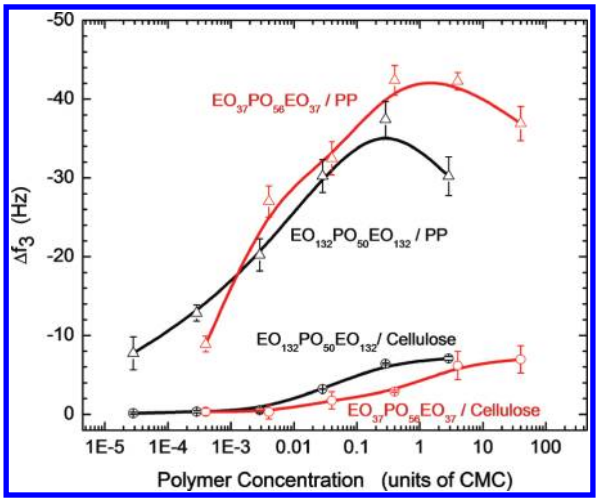

Figure 5. QCM frequency shift after adsorption from aqueous solutions of $EO_{37}PO_{56}EO_{37}$ and $EO_{132}PO_{50}EO_{132}$ on PP and cellulose after rinsing with water. Each data point represents the average of three independent measurements, each performed with a different surface at 25 ± 0.02 °C. The error bars represent experimental standard deviation. The solid lines are added as a guide to the eye.

found for the charged polymer). In contrast, relatively low adsorbed amounts were observed in experiments with hydrophilic silica and cellulose. In fact, in the case of silica and cellulose surfaces the adsorbed amount of $EO_{132}PO_{50}EO_{132}$ was negligible. The differences in adsorption can be explained by the effective interaction energies between the solid surface and the polymer blocks. For example, silica has higher affinity with PEO than with PPO segments [the interaction energies follow the following order from high to low values: PEO-silica > (PPO-silica, and PPO- polystyrene) > PEO-polystyrene].[29]

The loosely adsorbed molecules were removed upon rinsing with background solutions. The adsorbed amount on hydrophilic silica and cellulose for $DMAEMA_{24}-EO_{132}PO_{50}EO_{132}-DMAEMA_{24}$ was larger than that for $EO_{132}PO_{50}EO_{132}$. Electrostatic forces between the cationic PDMAEMA segments and the slightly anionic silica and cellulose surfaces are considered to be the main reason for the increased adsorption of PDMAEMA-capped polymers. The adsorbed amount of $DMAEMA_{24}-EO_{132}PO_{50}EO_{132}-DMAEMA_{24}$ was higher on silica surfaces compared to that on cellulose. This is likely due to higher surface charge density for silica.[33,34] Adsorption of $DMAEMA_{24}-EO_{132}PO_{50}EO_{132}-DMAEMA_{24}$ on hydrophobic PP surfaces was lower than that of $EO_{132}PO_{50}EO_{132}$. This behavior is likely due to the presence of PDMAEMA groups that tended to be solvated in water.

Figure 4d–f shows clearly non-Langmuirian adsorption isotherms with a maximum observed generally at polymer concentrations close to the cmc. A similar trend, with a maximum in adsorption, has been observed in the case of long chain alkanethiols[7] and other systems.[35] As was shown by Brandani and Stroeve, the reduction in rate of adsorption (as indicated in the present case by the negative of frequency shift) observed at the highest concentrations (specially distinctive in the case of PP surfaces) can be ascribed to a kinetically induced metastable equilibrium associated with progressively less efficient packing at the hydrophobic surface.[7]

The adsorption of $EO_{132}PO_{50}EO_{132}$ was compared with that of a polymer with relatively larger middle PPO block, such as $EO_{37}PO_{56}EO_{37}$ (see Figure 5). It was found that the adsorption of $EO_{132}PO_{50}EO_{132}$ at concentrations above the cmc was much lower on PP than that for $EO_{37}PO_{56}EO_{37}$ under similar conditions; however, no major differences in adsorption were observed on silica and cellulose surfaces (see Figure 5). These observations indicate the possibility that a relatively larger PEO block in $EO_{132}PO_{50}EO_{132}$ facilitated better solvation in the aqueous medium, which hindered adsorption. Compared to PEO, the hydrophobic PPO blocks have higher affinity for hydrophobic surfaces while the relatively larger PEO blocks tend to remain hydrated in water;[36] thus, the larger PPO/PEO ratio favors a more extensive adsorption on hydrophobic surfaces.

Viscoelasticity of Adsorbed $EO_{132}PO_{50}EO_{132}$ and $DMAEMA_{24}-EO_{132}PO_{50}EO_{132}-DMAEMA_{24}$ Layers. The QCM frequency shifts (Δf) observed upon adsorption of $EO_{132}PO_{50}EO_{132}$ and $DMAEMA_{24}-EO_{132}PO_{50}EO_{132}-DMAEMA_{24}$ were very distinctive for the different substrates with regard to the adsorbed amount and the kinetics of the process. These differences were attributed to the mass and structure of the polymer adsorbed layers, the relationship of which can be better discussed in the light of QCM's $\Delta D-\Delta f$ plots.

The changes in the slope of $\Delta D-\Delta f$ curves can shed some light on the various kinetic regimes and conformational changes occurring upon polymer adsorption.[37] The slope of the $\Delta D-\Delta f$ curves is related to the viscoelasticity of the adsorbed layer. For example, a straight line suggests the buildup of a homogeneous and relatively rigid layer. On the other hand, a curved profile may indicate variations in adsorbed polymer conformation with the degree of coverage. Figure 6 shows the QCM $\Delta D-\Delta f$ plots after adsorption of $EO_{132}PO_{50}EO_{132}$ and $DMAEMA_{24}-EO_{132}PO_{50}EO_{132}-DMAEMA_{24}$ from aqueous solution below (a and c) and above the cmc (b and d). The slopes of these curves for different substrates indicate that at submicellar concentrations both polymers tend to form a rigid adsorbed layer (Figure 6a,c). The "loops" in the $\Delta D-\Delta f$ profile are associated with the effect of rinsing with water. At high polymer concentrations (above cmc, Figure 6b,d), the $\Delta D-\Delta f$ plots indicate a more dissipative adsorbed layer. Two different regimes (slopes) were observed in the respective profiles for $EO_{132}PO_{50}EO_{132}$ adsorption on silica and PP. The results indicated an initial flat conformation followed by a steep increase in dissipation (viscoelasticity): $EO_{132}PO_{50}EO_{132}$ molecules first adsorbed onto the surfaces as a compact layer. As more polymers diffused to the interface, multiple layers may have been formed. In contrast, no variation in $\Delta D-\Delta f$ slope was observed for the adsorption on cellulose. Figure 6d indicates that $EO_{132}PO_{50}EO_{132}$ adsorption from solution at concentrations above the cmc on silica and PP surfaces followed two different regimes (two different slopes are observed in the $\Delta D-\Delta f$ profiles). The slope corresponding to the adsorption on PP is lower than that observed for cellulose. This is due to the conformation of the adsorbed polymer which adsorbed as a compact, less dissipative layer on PP. In the case of cellulose, $EO_{132}PO_{50}EO_{132}$ molecules first adsorbed onto the surfaces as a compact layer, but more polymers diffused to the interface and thicker layers were formed. Besides the lower charge density of cellulose, which leads to adsorption in a more extended (more dissipative) conformation, cellulose may respond to changes at the interface: it can swell or release water depending on the adsorbing species and the solvent. This does not apply to the case of the silica surface. The effect of surface charge and also the "responsiveness" of the surface make the measured dissipation much larger for cellulose than for silica.

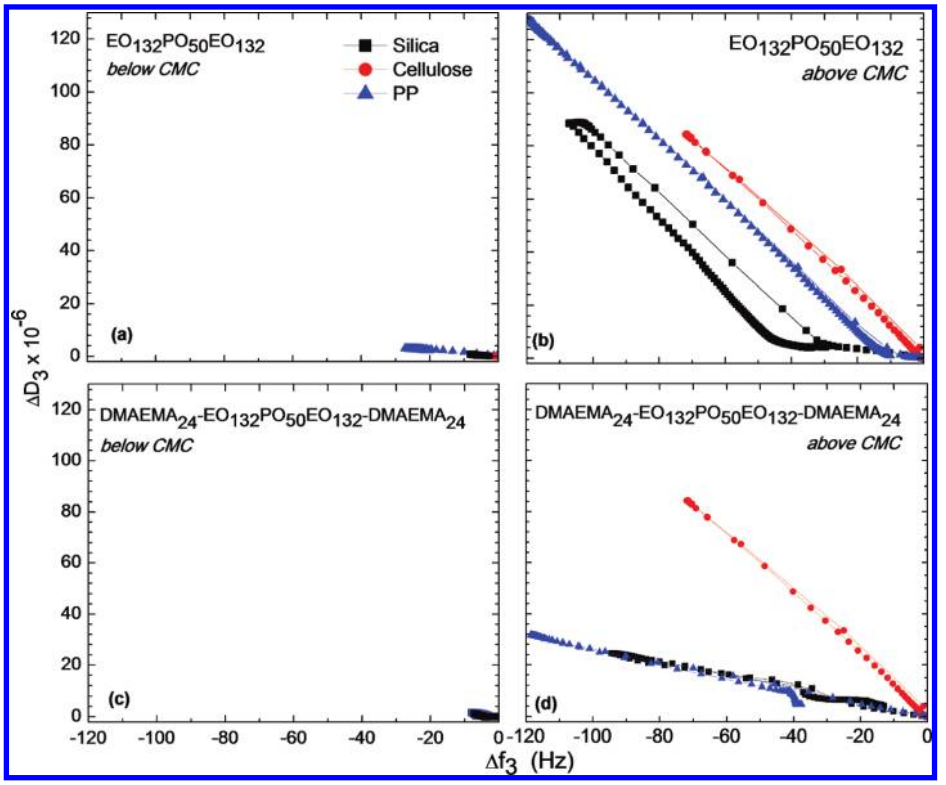

Figure 6. $\Delta D-\Delta f$ curves revealing changes in the conformation during adsorption of $EO_{132}PO_{50}EO_{132}$ and $DMAEMA_{24}-EO_{132}PO_{50}EO_{132}-DMAEMA_{24}$ from aqueous solution concentrations below (0.001%) (a and c) and above the cmc (10%) (b and d) on the different surfaces investigated at 25 ± 0.02 °C.

The respective buildup of the $EO_{132}PO_{50}EO_{132}$ and $DMAEMA_{22}-EO_{132}PO_{50}EO_{132}-DMAEMA_{22}$ layers from solution concentrations below and above the cmc and the changes observed after rinsing (irreversible adsorption) are shown more clearly in Figure S1, parts a, b and c, respectively (see Supporting Information). The molecules that remained at the interface after rinsing were expected to be bound more strongly.

A possible description of the buildup of soft adsorbed structure could include the formation of an initial thin patchy layer followed by an increased adsorbed mass as more molecules diffused to the interface, possibly forming loosely bound multilayers. Since the binding between these layers was expected to be weak, compared with the molecules in close vicinity to the surface, they could be removed easily by rinsing (see loops in the $\Delta D-\Delta f$ profiles). Upon rinsing, the $EO_{132}PO_{50}EO_{132}$ molecules that remained at the interface were expected to be bound more strongly on all surfaces. Despite such an effect, the values of energy dissipation for $DMAEMA_{24}-EO_{132}PO_{50}-EO_{132}-DMAEMA_{24}$ remained large after adsorption from solution concentration of 10% w/v, indicating that the polymers formed a large fraction of loops. As explained before, the high dissipation values may be linked to the large amount of water coupled in dangling PEO loops and tails[38,39] (see Figure S1 in Supporting Information).

Effect of Ionic Strength and Surface Charge Density on the Adsorption of $DMAEMA_{24}-EO_{132}PO_{50}EO_{32}-DMAEMA_{24}$. The ionic strength of the medium has an important influence on the electrostatic interactions between $DMAEMA_{24}-EO_{132}PO_{50}EO_{132}-DMAEMA_{24}$ and the different surfaces. To this end, the nature of the charge of the surface is critical in mediating interactions with the adsorbing polymer. QCM-D was used to investigate the effect of the ionic strength on adsorption of $DMAEMA_{24}-EO_{132}PO_{50}EO_{132}-DMAEMA_{24}$ on negatively charged silica[33,34] and uncharged PP[18,40] surfaces, as shown in parts a and b of Figure 7, respectively. At low ionic strengths, highly charged polyelectrolytes tend to exist in extended conformations, due to the repulsion between charged groups, while in relatively high ionic strength solutions polyelectrolytes tend to form more compact, Gaussian-like conformations.[41] Such effects are important also in adsorption on solid surfaces. As shown in Figure 8b, upon increasing the salt concentration from 0 to 1 M NaCl the adsorption of $DMAEMA_{24}-EO_{132}PO_{50}EO_{132}-DMAEMA_{24}$ on PP surfaces increased. The presence of salt in solution screened the repulsion between the cationic chains of $DMAEMA_{24}-EO_{132}PO_{50}EO_{132}-DMAEMA_{24}$, and therefore, the polymer molecules could adsorb with high surface densities.

Polymer adsorption on negatively charged surfaces was more complex (Figure 7a). With increasing salt concentration, up to 100 mM NaCl, the adsorption of $DMAEMA_{24}-EO_{132}PO_{50}-EO_{132}-DMAEMA_{24}$ increased. This can be ascribed to the effects already discussed for adsorption on uncharged PP surfaces. However, with further increases in salt concentration, e.g., at 1 M NaCl, polymer adsorption decreased. It has been reported that the thickness of the adsorbed layer can increase but the adsorbed amount may increase or decrease, depending on the nonelectrostatic polymer-surface affinity.[42] At high ionic strength cationic PDMADMA becomes more coiled, which reduces the available cationic sites for interaction with oppositely charged silica. Additionally, cationic PDMADMA segments extending from the surfaces are associated with counterions. The osmotic pressure associated with the concentration of counterions increases at high

dx.doi.org/10.1021/la201596x |*Langmuir* 2011, 27, 9769–9780

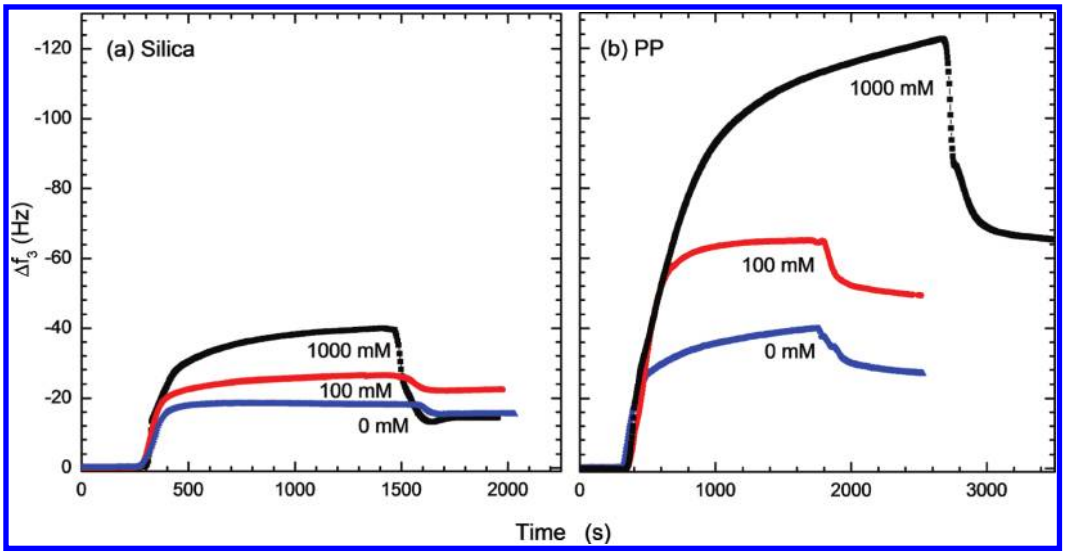

Figure 7. Mean values of third overtone QCM frequency as a function of time for $DMAEMA_{24}-EO_{132}PO_{50}EO_{132}-DMAEMA_{24}$ adsorption on silica (a) and PP (b) surfaces in aqueous solution concentrations of 0.1% w/v in water (0 mM NaCl), 100 mM NaCl and 1000 mM NaCl at 25 ± 0.02 °C. The experiments were conducted in an open (continuous) flow configuration with polymer solution injection rate of 0.1 mL/min (starting at about 300 s). The dip observed in all profiles soon after the adsorption plateau is associated with rinsing the system with water. Upon rinsing, abrupt changes in frequency were observed until reaching constant values.

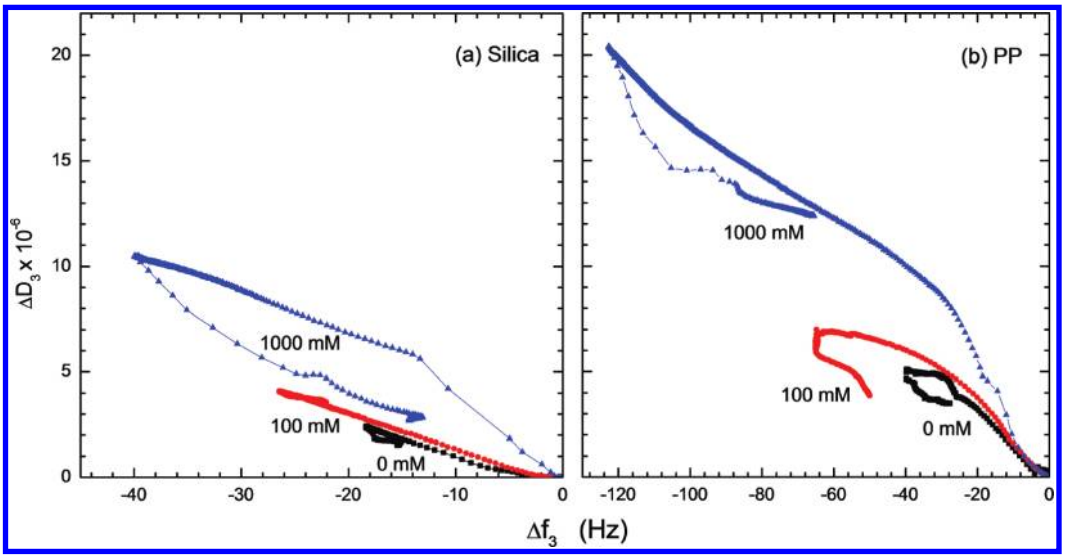

Figure 8. $\Delta D-\Delta f$ profiles revealing changes in the conformation during adsorption of $DMAEMA_{24}-EO_{132}PO_{50}EO_{32}-DMAEMA_{24}$ from solution concentration of 0.1% w/v on silica (a) and PP (b) surfaces at 25 ± 0.02 °C. NaCl concentrations are indicated as 0, 100, and 1000 mM.

ionic strength and a large amount of coupled water may be excluded from the adsorbed polymer layer.

Figure 8 illustrates the changes in energy dissipation as a function of the shift in frequency upon adsorption of $DMAEMA_{24}-EO_{132}PO_{50}EO_{132}-DMAEMA_{24}$ from aqueous solution at different background NaCl concentrations. The dissipation and frequency profiles were linear for polymer adsorbing from pure water or low ionic strength solution. In contrast, adsorption from high ionic strength solutions showed a $\Delta D-\Delta f$ slope that changed with the frequency shift. This indicated that, contrary to the case of low ionic strengths, conformational changes occurred upon adsorption from solutions of high NaCl concentrations. It is possible that adsorption occurred as a single layer from low ionic strength solution, while multilayers or more complex polymer structures formed when adsorbing at high ionic strength. Furthermore, the steep slope of the $\Delta D-\Delta f$ profiles was closely related to electrostatic effects that induced (1) a reduction in the number of directly surface-bound segments and (2) an increased length and fraction of loops and tails of the adsorbed PDMAEMA groups. The "loops" in the $\Delta D-\Delta f$ profile indicated the effect of water rinsing and associated reduction in dissipation. Finally, there was an indication of a more compact, less viscoelastic adsorbed $DMAEMA_{24}-EO_{132}PO_{50}EO_{132}-DMAEMA_{24}$ layer remaining on the negatively charged silica surfaces.

The slope in the $\Delta D-\Delta f$ profiles shown in Figure 8 became much steeper with increasing salt concentration. However, the

dx.doi.org/10.1021/la201596x |*Langmuir* 2011, 27, 9769–9780

conformation of polymer layers adsorbed on PP might be quite different than that on silica due to the nature of the interactions driving the adsorption of $DMAEMA_{24}-EO_{132}PO_{50}EO_{132}-DMAEMA_{24}$.

Figure 9 shows changes in refractive index obtained by SPR after adsorption of $DMAEMA_{24}-EO_{132}PO_{50}EO_{32}-DMAEMA_{24}$ from aqueous solutions of different ionic strengths on PP surfaces. In these experiments, after a stable intensity baseline was obtained, $DMAEMA_{24}-EO_{132}PO_{50}EO_{132}-DMAEMA_{24}$ was injected, and data were collected until a plateau value was reached. Background solution (water or electrolyte solution) was then injected to rinse out any loosely adsorbed polymers. As was the case in QCM experiments (Figure 7b), the change in refractive index, which is related to the adsorbed amount of $DMAEMA_{24}-EO_{132}PO_{50}EO_{132}-DMAEMA_{24}$, increased with increasing salt concentration. In general, both QCM and SPR experiments showed similar trends.

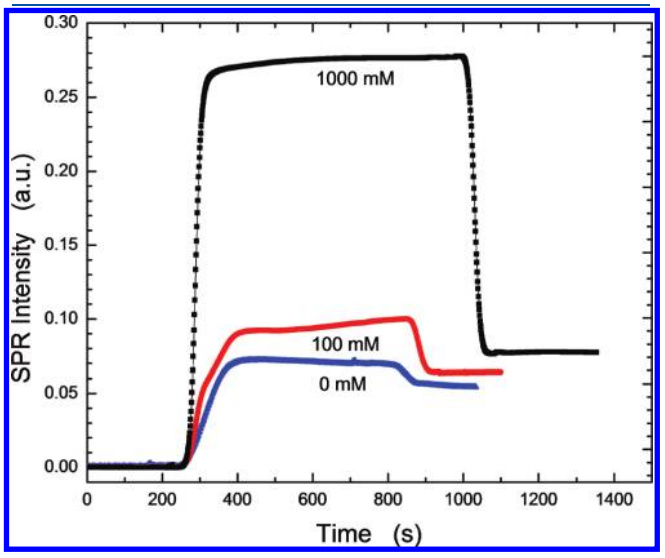

Figure 9. Changes in SPR intensity as a function of time after adsorption of $DMAEMA_{24}-EO_{132}PO_{50}EO_{132}-DMAEMA_{24}$ on PP under the same conditions as those used in QCM experiments shown Figure 8. NaCl concentrations are indicated as 0, 100, and 1000 mM.

Effect of Temperature on Adsorption of $DMAEMA_{24}-EO_{132}PO_{50}EO_{132}-DMAEMA_{24}$. Figure 10 shows data pertaining to the adsorption of $DMAEMA_{24}-EO_{132}PO_{50}EO_{132}-DMAEMA_{24}$ on PP surfaces at 40 °C obtained from QCM and SPR measurements. The adsorption isotherms followed similar trends as those observed at 25 °C; the amount of adsorbed polymer increased with increasing salt concentration. Table 3 lists the mass of $DMAEMA_{24}-EO_{132}PO_{50}EO_{132}-DMAEMA_{24}$ adsorbed on PP surfaces from aqueous solution with different salt concentrations (at 25 and 40 °C). The adsorbed amount increased with solution ionic strength; additionally, it was expected that the cationic polymer became more compact (as also evidenced by the light scattering data measured under the same condition; see Table 1). Electrostatic screening reduced the repulsion forces between the cationic PDMAEMA chains and as a result more molecules adsorbed on the surface. The adsorbed amount calculated from the QCM experiments was higher than the values obtained by SPR, due to the effect of water coupling detected in QCM. The amount of $DMAEMA_{24}-EO_{132}PO_{50}-EO_{132}-DMAEMA_{24}$ adsorbed on PP surfaces at 40 °C was higher than that measured at 25 °C because the polymer became more compact with increased temperature, as supported by the light scattering results (see Table 1). The extent of surface coverage at saturation at the PP-liquid interfaces (≈31 and 40 nm^2/molecule obtained by QCM and SPR, respectively) was much lower, as expected, when compared with results obtained at the air−liquid interface, where a tight packing was observed (1.6 nm^2/molecule from surface tension data). This is likely due to the higher configurational entropic penalty sustained by the copolymers at solid surfaces compared to the more diffuse air−water interface.

The differences observed in the QCM and SPR results can be ascribed to the contribution of coupled water (trapped, hydration, and solvation water) associated with ethylene oxide (EO) and the cationic PDMAEMA groups. The amount of water coupled in the adsorbed layer was calculated by using eq 4 as a function of salt concentration and temperature. The amount of

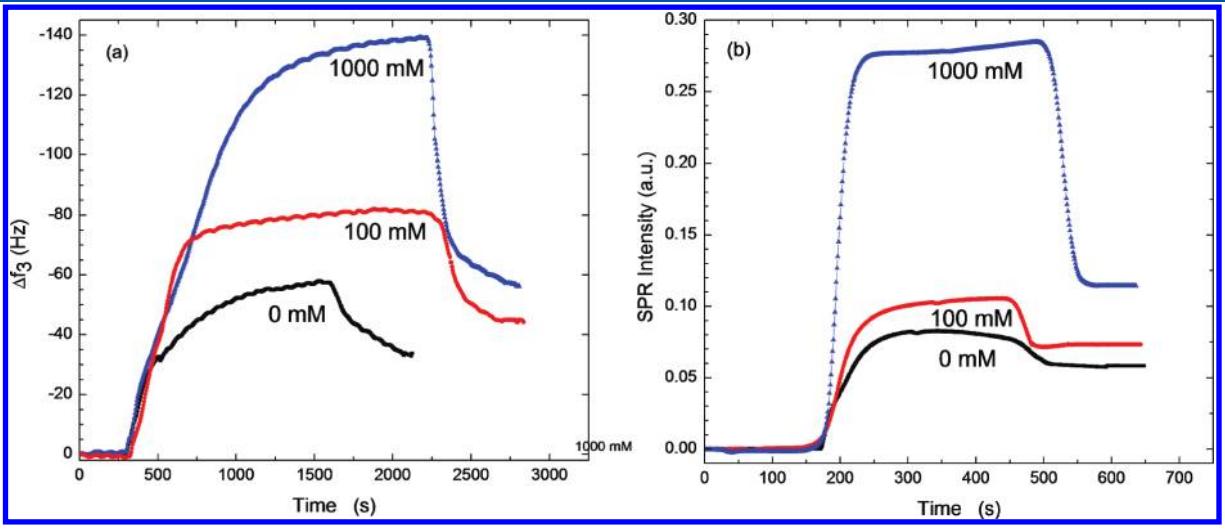

Figure 10. Third overtone QCM frequency and SPR intensity shifts as a function of time upon adsorption of $DMAEMA_{24}-EO_{132}PO_{50}-EO_{132}-DMAEMA_{24}$ on PP surfaces from aqueous solution concentrations of 0.1% w/v from water (black), 100 mM NaCl (red), and 1000 mM NaCl (blue) at 40 °C. The increase of Δf and intensity observed in all profiles soon after the adsorption plateau resulted from rinsing the system with water.

dx.doi.org/10.1021/la201596x |*Langmuir* 2011, 27, 9769–9780

Table 3. $DMAEMA_{24}-EO_{132}PO_{50}EO_{132}-DMAEMA_{24}$ Adsorbed Mass (QCM and SPR) from 0.1% w/v Solution Concentration on PP Surfaces at Different Ionic Strengths and Temperatures

	25 °C			40 °C		
[NaCl], mM	Δm_{QCM}, ng/cm^2	Δm_{SPR}, ng/cm^2	% water (eq 4)	Δm_{QCM}, ng/cm^2	Δm_{SPR}, ng/cm^2	% water (eq 4)
0	171	134	22	196	167	15
100	215	181	16	265	229	14
1000	291	252	14	336	306	9

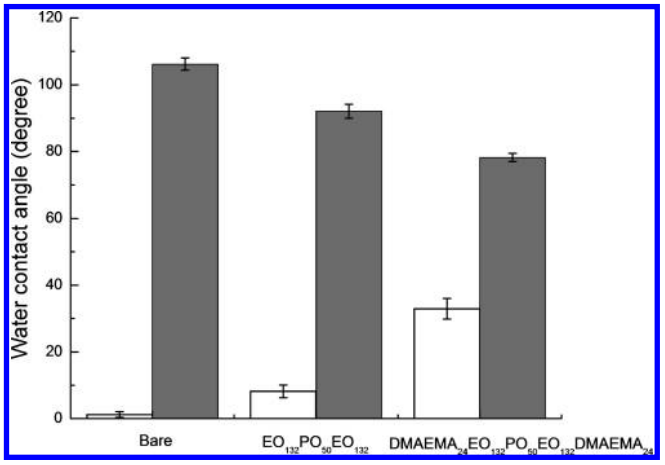

Figure 11. Water contact angle (WCA) of PP (filled bars) and silica (unfilled bars) before (bare surfaces) and after adsorption of $EO_{132}PO_{50}EO_{132}$ and $DMAEMA_{24}-EO_{132}PO_{50}EO_{132}-DMAEMA_{24}$ from 0.1% aqueous solutions (experiments were performed at room temperature and under the same relative humidity conditions).

coupled water decreased from 22 to 14% with increasing ionic strength, probably due to the release of water molecules from the adsorbed polymers.

Changes in Water Contact Angle after Polymer Adsorption. Figure 11 shows the advancing water contact angles (WCA) on PP and silica surfaces before and after immersion in 0.1% $EO_{132}PO_{50}EO_{132}$ and $DMAEMA_{24}-EO_{132}PO_{50}EO_{132}-DMAEMA_{24}$ aqueous solutions. Bare PP surfaces showed relatively high advancing contact angles (≈106°). After adsorption of $EO_{132}PO_{50}EO_{132}$ and $DMAEMA_{24}-EO_{132}PO_{50}EO_{132}-DMAEMA_{24}$, the WCA was reduced by ≈14° and ≈28°, respectively (due to the hydrophilic EO and highly water-soluble PDMAEMA segments attached on the surfaces). This limited reduction in WCA can be explained by the relatively low adsorption density for these polymers. Adsorption of $EO_{132}PO_{50}EO_{132}$ on silica surfaces had little effect on the WCA, while adsorption of $DMAEMA_{24}-EO_{132}PO_{50}EO_{132}-DMAEMA_{24}$ increased the contact angle of silica to 32°, indicating a large density of exposed PPO blocks upon adsorption (Figure 4d).

CONCLUSIONS

Triblock copolymers of PEO−PPO−PEO type have attracted attention in various applications due to their amphiphilic nature and their capability to produce functional coatings on solid substrates. In this study, $EO_{132}PO_{50}EO_{132}$ with or without end-caps consisting of cationic chains of poly(2-dimethylaminoethyl methacrylate) (PDMAEMA) were applied on PP, cellulose, and silica. The surface activity of the tested polymers, $EO_{132}PO_{50}EO_{132}$ and $DMAEMA_{24}-EO_{132}PO_{50}EO_{132}-DMAEMA_{24}$, and their adsorption behavior on the substrates with different hydrophilicity were investigated by using QCM and SPR. Adsorption of $EO_{132}PO_{50}EO_{132}$ and $DMAEMA_{24}-EO_{132}PO_{50}EO_{132}-DMAEMA_{24}$ depended highly on the nature of the surface, likely due to the different interactions driving the adsorption process. Solvency and electrostatic forces were primary factors influencing adsorption on hydrophilic silica and cellulose surfaces, while hydrophobic effects played a key role in the case of hydrophobic PP. Adsorption of $DMAEMA_{24}-EO_{132}PO_{50}EO_{132}-DMAEMA_{24}$ on uncharged PP surfaces increased with solution ionic strength, while an adsorption maximum was found for silica. This was explained in terms of (a) a more coiled conformation at high salt concentrations, (b) electrostatic interactions between ions associated with the cationic PDMAEMA groups and the negatively charged silica surfaces, and (c) a large amount of water excluded from the adsorbed layer.

Adsorption of $DMAEMA_{24}-EO_{132}PO_{50}EO_{132}-DMAEMA_{24}$ at relatively high temperatures (40 °C) was higher than at 25 °C due to aggregation of PPO segments. Finally, adsorption of a small amount of $DMAEMA_{24}-EO_{132}PO_{50}EO_{132}-DMAEMA_{24}$ reduced the water contact angle of PP, to a large extent due to the highly soluble cationic PDMAEMA group. For silica the WCA was increased due to the high density of PPO segments exposed to water.

ASSOCIATED CONTENT

Supporting Information. $\Delta D-\Delta f$ data after rinsing adsorbed $EO_{132}PO_{50}EO_{132}$ and $PDM_{24}-EO_{132}PO_{50}EO_{132}-PDM_{24}$ from solution concentrations below and above the cmc. This material is available free of charge via the Internet at http://pubs.acs.org.

AUTHOR INFORMATION

Corresponding Author

*E-mail: ojrojas@ncsu.edu. Tel: +1-919-513 7494. Fax: +1-919-515 6302.

ACKNOWLEDGMENT

This project was supported by NC State University Nonwovens Cooperative Research Center under Project number 07-98.

REFERENCES

(1) *BASF Technical Data Sheet*; BASF Co.: Parsippany, NJ, 1989.

(2) Muller, R. H. In *Colloidal Carriers for Controlled Drug Delivery and Targeting*; Muller, R. H.; Ed.; CRC Press: Boca Raton, FL, 1991; p 23.

(3) Cosgrove, T. *J. Chem. Soc. Faraday Trans.* **1990**, *86*, 1323.
(4) Malmsten, M.; Linse, P.; Cosgrove, T. *Macromolecules* **1992**, *25*, 2474–2481.
(5) Shar, J. A.; Obey, T. M.; Cosgrove, T. *Colloids Surf.* **1998**, *136*, 21–33.
(6) Brandani, P.; Stroeve, P. *Macromolecules* **2004**, *37*, 6640–6643.
(7) Brandani, P.; Stroeve, P. *Macromolecules* **2003**, *36*, 9492–9501.
(8) Liu, X.; Wu, D.; Turgman-Cohen, S.; Genzer, J.; Theyson, T.; Rojas, O. *J. Langmuir* **2010**, *26*, 9565–9574.
(9) Chen, W.-Y.; Alexandridis, P.; Su, C.-K.; Patrickios, C. S.; Hertler, W. R.; Hatton, T. A. *Macromolecules* **1995**, *28*, 8604–8611.
(10) Baines, F. L.; Armes, S. P.; Billingham, N. C.; Tuzar, Z. *Macromolecules* **1996**, *29*, 8151–8159.
(11) Cho, S. H.; Jhon, M. S.; Yuk, S. H.; Lee, H. B. *J. Polym. Sci.; Part B* **1997**, *35*, 595–598.
(12) Lin, J.; Qiu, S.; Lewis, K.; Klibanov, A. M. *Biotechnol. Prog.* **2002**, *18*, 1082–1086.
(13) Cheng, Z.; Zhu, X.; Shi, Z. L.; Neoh, K. G.; Kang, E. T. *Ind. Eng. Chem. Res.* **2005**, *44*, 7098–7104.
(14) Lee, S. B.; Koepsel, R. R.; Morley, S. W.; Matyjaszewski, K.; Sun, Y.; Russell, A. *J. Biomacromolecules* **2004**, *5*, 877–882.
(15) Nurmi, L.; Holappa, S.; Nykänen, A.; Laine, J.; Ruokolainen, J.; Seppälä *J. Polymer* **2009**, *50*, 5250–5261.
(16) Vesterinen, A.; Lipponen, S.; Rich, J.; Seppala, J. *Express Polym. Lett.* **2011**, *5*, 754–765.
(17) Vesterinen, A.; Rich, J.; Myllytie, P.; Laine, J.; Seppälä, *J. Macromol Mater. Eng* **2010**, *295*, 269–275.
(18) Song., J.; Liang, J.; Liu, X.; Krause, W. E.; Hinestroza, J. P.; Rojas, O. *J. Thin Solid Films* **2009**, *517*, 4348–4354.
(19) Homola, J.; Yee, S. S.; Gauglitz, G. *Sens. Actuators B* **1999**, *54*, 3–15.
(20) Liedberg, B.; Nylander, C.; Lundstrom, I. *Biosens. Bioelectron.* **1995**, *10*, R1–R9.
(21) Rodahl, M.; Kasemo, B. *Sens. Actuators A* **1996**, *54*, 448–456.
(22) Foster, B.; Cosgrove, T.; Hammouda, B. *Langmuir* **2009**, *25*, 6760–6766.
(23) Reimhult, E.; Larsson, C.; Kasemo, B.; Ho1o1k, F. *Anal. Chem.* **2004**, *76*, 7211–7220.
(24) Fei, S. Affinity Interaction between Hexamer Peptide Ligand HWRGWV and Immunoglobulin G Studied by Quartz Crystal Microbalance and Surface Plasmon Resonance. Ph.D. Thesis, North Carolina State University, 2009.
(25) Höök, F.; Kasemo, B. *Anal. Chem.* **2001**, *73*, 5796–5804.
(26) Alexandridis, P.; Holzwarth, J. F.; Hatton, T. A. *Macromolecules* **1994**, *27*, 2414–2425.
(27) Nolan, S. L.; Philips, R. J.; Cotts, P. M.; Dungan, S. R. *J. Colloid Interface Sci.* **1997**, *191*, 291–302.
(28) Jhon, Y. K.; Bhat, R. R.; Jeong, C.; Rojas, O. J.; Szleifer, I.; Genzer, J. *Macromol. Rapid Commun.* **2006**, *27*, 697–701.
(29) Shar, J. A.; Obey, T. M.; Cosgrove, T. *J. Colloid Surf. A* **1999**, *150*, 15–23.
(30) Char, K.; Cast, A. P.; Frank, C. W. *Langmuir* **1988**, *4*, 989.
(31) Char, K.; Frank, C. W.; Gast, A. P. *Langmuir* **1990**, *6*, 767.
(32) Levitz, P.; van Damme, H.; Keravis, D. *J. Phys. Chem.* **1984**, *88*, 2228.
(33) Radtchenko, I. L.; Papastavrou, G.; Borkovec, M. *Biomacromolecules* **2005**, *6*, 3057–3066.
(34) Rodrigues, F. A.; Monteiro, P. J. M.; Sposito, G. *J. Colloid Interface Sci.* **1999**, *211*, 408–409.
(35) Munch, M. R.; Gast, A. P. *J. Chem. Soc. Faraday Trans.* **1990**, *86*, 1341–1348.
(36) Green, R. J.; Tasker, S.; Davies, J.; Davies, M. C.; Roberts, C. J.; Tendler, S. J. B. *Langmuir* **1997**, *13*, 6510–6515.
(37) Su, X. D.; Zong, Y.; Richter, R.; Knoll, W. *J. Colloid Interface Sci.* **2005**, *287*, 35–42.
(38) Dahlgren, M. A. G.; Hollenberg, H. C. M.; Claesson, P. M. *Langmuir* **1995**, *11*, 4480–5.
(39) Claesson, P. M. In *Colloid—Polymer Interactions: From Fundamentals to Practice*; Dubin, P., Farinato, R.; Eds; John Wiley and Sons: New York, 1999.
(40) Meagher, L.; Pashley, R. M. *Langmuir* **1995**, *11*, 4019–4024.
(41) Ullner, M.; Woodward, C. E. *Macromolecules* **2002**, *35*, 1437–45.
(42) Linse, P. *Macromolecules* **1996**, *29*, 326–36.